13th World Conference on Earthquake Engineering
Vancouver, B.C., Canada
August 1-6, 2004
Paper No. 3481

ENERGY DISSIPATION CAPACITY OF FLEXURE-DOMINATED REINFORCED CONCRETE MEMBERS

H. PARK[1] and T. EOM[2]

SUMMARY

As advanced earthquake analysis/design methods are developed, it is required to estimate precisely the cyclic behavior of reinforced concrete members that is characterized by strength, deformability, and energy dissipation capacity. However, presently, energy dissipation capacity is estimated by either empirical equations which are not sufficiently accurate, or experiments and sophisticated numerical analysis which are difficult to use in practice. In the present study, nonlinear finite element analysis was performed to investigate the behavioral characteristics of flexure-dominated RC members under cyclic load. Based on the investigation, a simplified method to estimate the energy dissipation capacity of flexure-dominated member was developed, and was verified by the comparisons with existing experiments on beams, columns, and structural wall. The proposed method can accurately estimate the energy dissipation capacity of the member considering various design variables such as reinforcement ratio and arrangement, axial compression, and sectional shape, though the overall cyclic curve complicated by the stiffness degradation and pinching is not known. An example of nonlinear static and dynamic analysis using the proposed method was presented.

INTRODUCTION

Recently, performance-based methods for earthquake design were developed. [1, 2] To use such advanced methods, it is necessary to estimate precisely the cyclic behavior of structural members which is represented by three primary ingredients: strength, deformability, and energy dissipation capacity (per load cycle) (Fig. 1). Generally, reinforced concrete members show complex cyclic behavior with stiffness degradation and pinching. Therefore, the evaluation of seismic performance of RC members is usually limited to strength and deformability. The estimation of energy dissipation capacity depends on empirical equations that are not sufficiently accurate, or on nonlinear numerical analysis that is difficult to use.

For example, in the Capacity-Spectrum-Method of ATC-40 [1], a nonlinear static analytical method, structures are classified into three categories according to their expected capacity of energy dissipation. The energy dissipation capacity E_{kh} is obtained by assuming that the structure displays a linearized kinematic hardening behavior (Fig. 2). Then, the actual energy dissipation capacity E_D is calculated by

[1] Associate Prof., Dep. of Archit., Seoul Nat. Univ., Seoul, Korea. Email:parkhg@snu.ac.kr
[2] Graduate Stud., Dep. of Archit., Seoul Nat. Univ., Seoul, Korea. Email:macraian@snu.ac.kr

multiplying the empirical ratios of 0.33, 0.67, or 1.0 to E_{kh} which is prescribed by the category of the structure. Generally, energy dissipation capacity depends on various parameters such as reinforcement ratio, arrangement of reinforcing bars, and shape and size of the members' cross-sections. Therefore, such empirical methods cannot precisely estimate the energy dissipation capacity, and as a result, they reduce the overall accuracy of the evaluation method. For economical and safe seismic design, simple but sufficiently accurate methods for estimating energy dissipation capacity are needed.

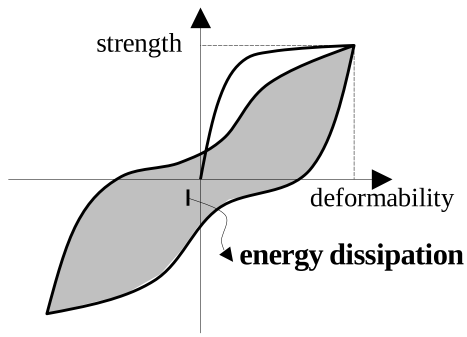

Fig. 1 Cyclic behavior of R/C members; strength, deformability, and energy dissipation

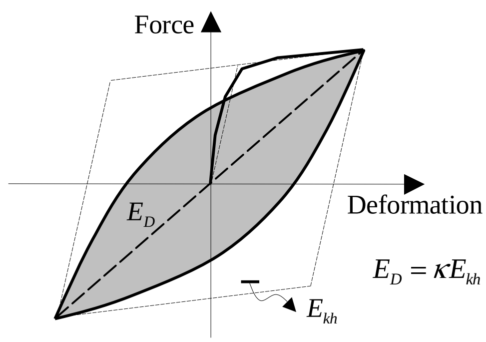

Fig. 2 Definition of energy dissipation by ATC-40 [1]

ENERGY DISSIPATION CAPACITY OF REINFORCED CONCRETE MEMEBRS

A reinforced concrete member dissipates energy by experiencing inelastic behavior during cyclic loading. Since the reinforced concrete member is composed of concrete and reinforcing steel, its energy dissipation can be defined by the sum of the energy dissipated by concrete and reinforcing steel.

$$E_{\mathrm{D}} = E_{\mathrm{concrete}} + E_{\mathrm{steel}} \tag{1}$$

where E_{D} = total energy dissipated by the reinforced concrete member during cyclic loading, E_{concrete}, E_{steel} = the energy dissipated by concrete and reinforcing steel, respectively.

Fig. 3 shows the cyclic behavior of plain concrete and reinforcing steel. [3, 5] Concrete is a brittle material composed of aggregates and matrix. Therefore, if cyclic loading is repeated at a specific displacement, concrete dissipates considerably less energy than reinforcing steel exhibiting plastic behavior does, as observed in many experiments.(see Fig. 3 (a)) [3, 4] For the reason, the overall dissipated energy of the member is equivalent to the sum of the energy dissipated by flexural re-bars arranged in the member.

$$E_{\mathrm{D}} \cong E_{\mathrm{steel}} \tag{2}$$

However, it should be noted that for the member subjected to excessively high axial compressive load, concrete dissipates considerable energy because a large volume of concrete contributes to resist the axial load.

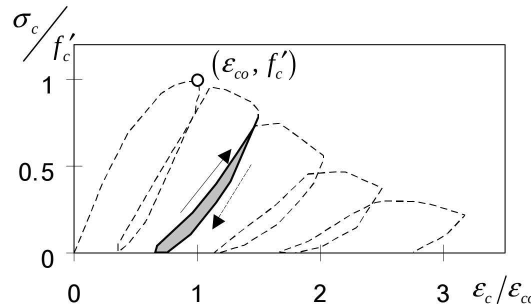

(a) Cyclic compression test of conrete [3]

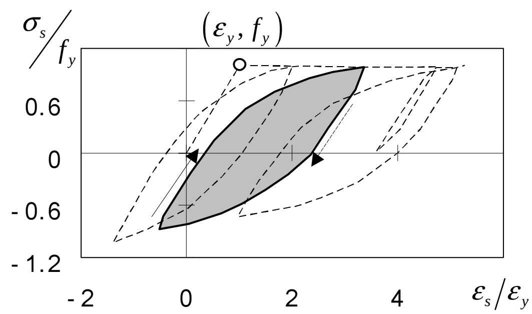

(b) Cyclic stress-strain curve [5]

Fig. 3 Cyclic behavior of concrete and re-bar

If Eq. (2) is acceptable, the overall energy dissipation capacity of the reinforced concrete member can be evaluated using the energy dissipated by re-bars without knowing the complex cyclic behavior. The energy dissipated by re-bars can be calculated with the amount of re-bars and the differential strains which the re-bars experience during cyclic loading.

STRAIN HISTORY OF RE-BARS

To evaluate the energy dissipated by re-bars, the differential strains that the re-bars experience during cyclic loading must be estimated. Nonlinear FE analyses for reinforced concrete members subject to cyclic loading were performed to investigate the hysteretic behavior of re-bars. The computer program developed by Park and Klingner [6] was used in the numerical study.

As shown in Fig. 4, in flexure-dominated members, most of the inelastic deformation is developed in the plastic hinges during cyclic loading, and the contribution of shear force can be neglected. Therefore, the wall-column model subject to uniform bending moment and axial compression as shown in Fig. 4 were selected.

Table 1 presents dimensions and properties of W1 and W2. No shear force was applied to the specimens. Therefore, the behaviors of the specimens were not affected by shear force. W1 was subject to uniform bending moment without axial compression force applied. W3 had the same number of re-bars as W1 and was subject to axial compressive force $0.1 f_c' A_g$. Since the axial force increases the moment-carrying capacity for the member subject to low compressive force, the moment carrying capacity of W3 is larger than that of W1.

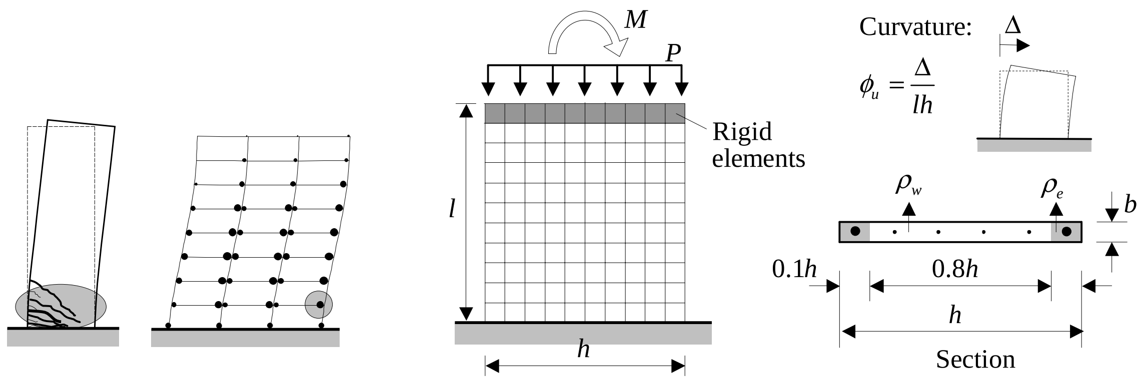

Fig. 4 Finite element model for plastic hinge of wall-column

Table 1 Dimension and properties of models for numerical analysis

Specimen	Length l mm	Depth h mm	Width b mm	Reinforcement Ratio (%)			Axial Force $P/A_g f_c'$	Compressive Strength of Concrete f_c' MPa	Yield Strength of Re-bar f_y MPa	Dissipated Energy e_D kN
				Total ρ	Ends ρ_e	Middle ρ_w				
W1	4400	4000	160	1.02	4.30	0.2	0.00	24	400	22.3
W2	4400	4000	160	1.02	4.30	0.2	0.10	24	400	24.2

Fig. 5 compares the cyclic moment-curvature curves of the specimens. W1 that was not subject to axial compression does not show pinching. On the other hand, W2 show the complicated behavior due to stiffness degradation and pinching. In this figure, the reference points where the cyclic curves are characterized by changes in strength and stiffness were marked A through H.

Fig. 6 shows the cyclic stress-strain relations of re-bars at the ends and the middle of the cross-section obtained at reference points A through H. Approximately, the maximum and minimum strains for the two specimens occurred at A, C(or G), and E. As shown in Fig. 6, the boundaries of the cross-section have the maximum and the minimum strains at A and E, and during one load cycle, one cycle of energy dissipation occurs. On the other hand, the web of the cross-section experiences two cycles of energy dissipation, which have the maximum and the minimum at A and C, and at E and G, respectively. As shown in the figure, the differential strains of the boundary re-bars for W1 and W2 are the same, regardless of whether axial force is applied to the member or not. On the other hand, due to the effect of the axial force, the differential strains of the webs are different.

However, generally, both the amount of re-bars and the differential strains in the webs are less than those in the boundaries. Furthermore, if the differential strain is less than two times the yield strain, the re-bars remain elastically, and do not dissipate energy. For the reasons, conservatively, the contribution of the re-bars in the web can be neglected, which means that the effect of axial force on the energy dissipation capacity can be neglected. This is confirmed by the fact that the energy dissipation capacities of W1 and W2 presented in Table 1 are almost identical. Therefore, the energy dissipation capacity of a flexure-dominated member can be calculated using the hypothetical cross-section subject to pure bending, neglecting the compressive force actually applied.

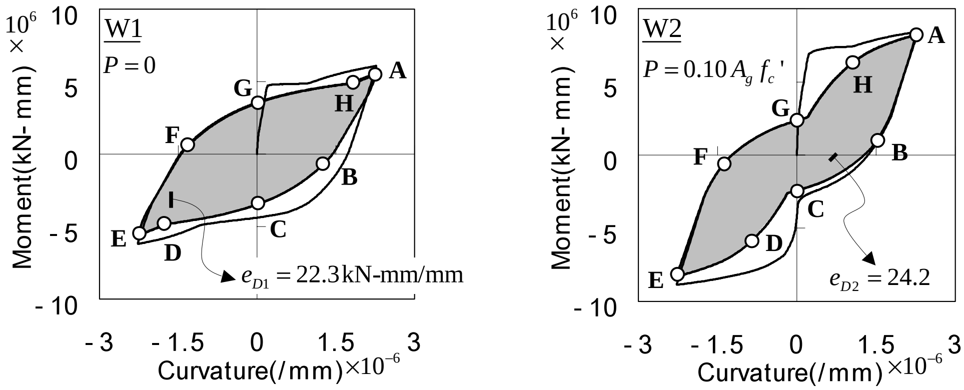

Fig. 5 Cyclic curves of wall-column Models

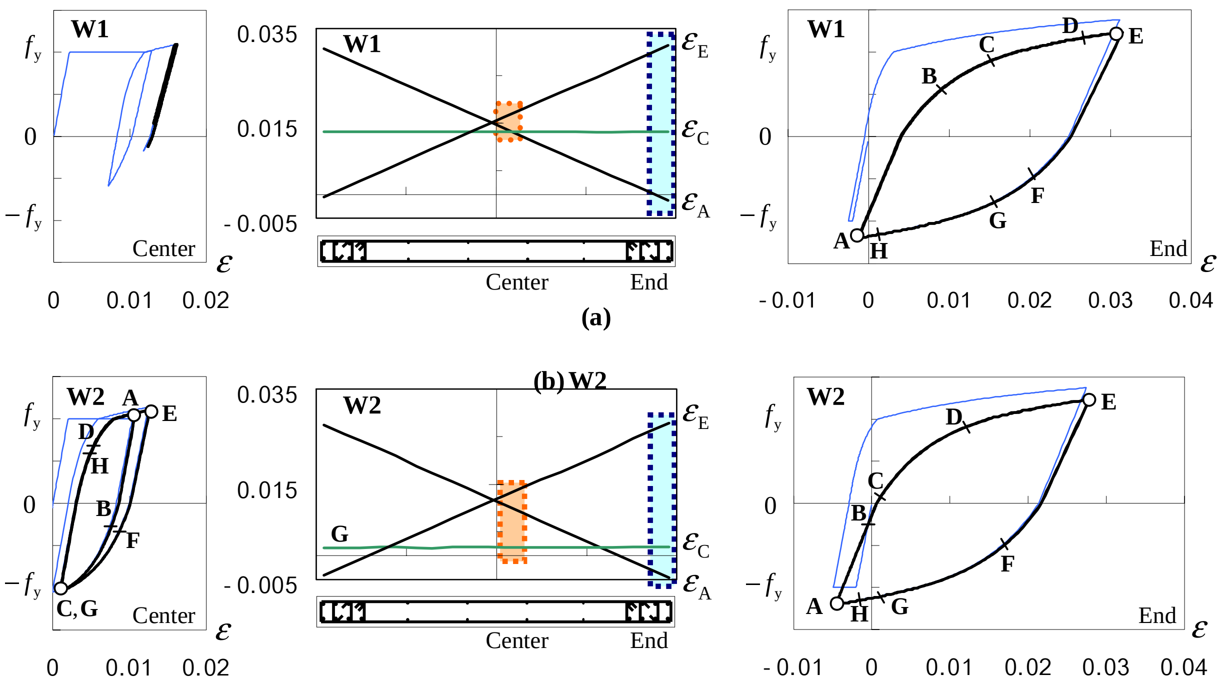

Fig. 6 Hysteretic stress-strain relation of re-bars at the ends and the middle of the section: (a) W1 not subject to axial compression; (b) W2 subject to axial compression

EVALUATION OF ENERGY DISSIPATION CAPACITY

As shown in Fig. 7, energy dissipated by a unit volume of re-bar for maximum and minimum strains can be calculated as follows.

$$U_D = 2R_B f_y \left(\varepsilon_1 - \varepsilon_2 - 2\varepsilon_y\right) \quad (3)$$

where, f_y, ε_y = yield stress and strain of reinforcing steel, ε_1, ε_2 = maximum and minimum strains, R_B = reduction factor representing the Bauschinger effect, which is approximately set to 0.75. [5] Since the re-bar does not dissipate energy in the elastic range, U_D is equal to zero if $\varepsilon_1 - \varepsilon_2 - 2\varepsilon_y < 0$.

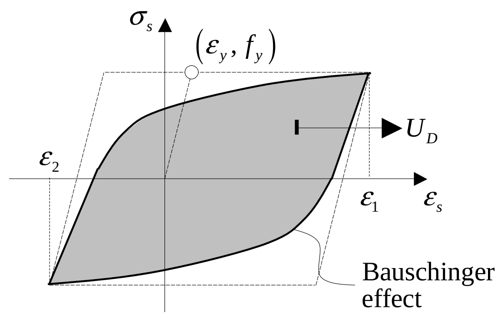

Fig. 7 Strain energy density of re-bars

Energy Dissipated during Cyclic Loading

Fig. 8 shows profiles of maximum and minimum strains for a rectangular cross-section with symmetric re-bar arrangement, developed during cyclic loading. For convenience in calculation, the strain profiles were simplified, neglecting the complex behavior occurring in the web, which did not significantly affect the overall energy dissipation capacity as explained in **STRAIN HISTORY OF RE-BARS**. To develop a simple equation, as shown in the figure, the re-bars were idealized as uniformly distributed re-bars with reinforcement ratio ρ_w and boundary re-bars with cross-sectional area A_s arranged at both ends. For the distributed re-bars, the differential strain at a distance x from the centroid of the cross section is $2\phi_u x$, and U_D is calculated by substituting $2\phi_u x$ for $\varepsilon_1 - \varepsilon_2$ in Eq. (3).

However, the re-bars located in $0 \le x \le \varepsilon_y/\phi_u$ remain elastically and do not dissipate energy: U_D should be zero for $0 \le x \le \varepsilon_y/\phi_u$. U_D of the boundary re-bars is obtained by substituting $(2\phi_u)(h_s/2)$ for $\varepsilon_1 - \varepsilon_2$ in Eq. (3). The dissipated energy e_D of a rectangular cross-section can be calculated by integrating the energy density U_D over the entire cross-section.

$$\begin{aligned} e_D &= \int_A U_D \rho(x)\, dA \\ &= 2R_B\left(2 f_y\right)\int_{\varepsilon_y/\phi_u}^{h/2}\left(2\phi_u x - 2\varepsilon_y\right)\rho_w dx + 2R_B\left(2 f_y\right)\left(2\phi_u \frac{h_s}{2} - 2\varepsilon_y\right) A_s \end{aligned} \tag{4}$$

where ρ = reinforcement ratio for total re-bars, b, h = width and depth of the rectangular cross-section, ϕ_u = maximum curvature, and h_s = distance between the re-bar layers located at the boundaries. In Eq. (4), the first and second terms represent the energy dissipated by the distributed re-bars and the boundary re-bars, respectively. Eq. (4) can be redefined with $p = \rho_w/\rho$ (see Fig. 8):

$$e_D = 4R_B \rho f_y b h^2 \phi_u \left[(1-p)\left(\frac{1}{2}\frac{h_s}{h} - \frac{\varepsilon_y}{\phi_u h}\right) + p\left(\frac{1}{2} - \frac{\varepsilon_y}{\phi_u h}\right)^2 \right] \tag{5}$$

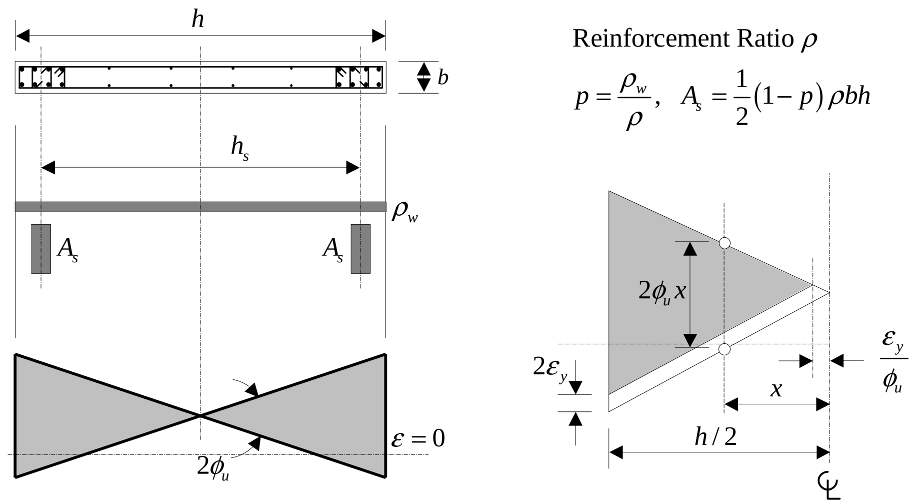

Fig. 8 Evaluation of energy dissipation capacity for the cross-section

Eq. (5) was derived assuming symmetric cyclic behavior in positive and negative directions. If the member is subjected to asymmetric cyclic behavior, the energy dissipation capacity can be obtained using the average curvature in two opposite directions.

Like the rectangular section, for the circular section and for the beam or T-beam with asymmetric re-bar arrangement, the energy dissipation capacity can be estimated using the differential strains of re-bars.

The energy dissipation capacity E_D of a plastic hinge is calculated as (Fig. 9)

$$E_D = e_D\, l_p \tag{6}$$

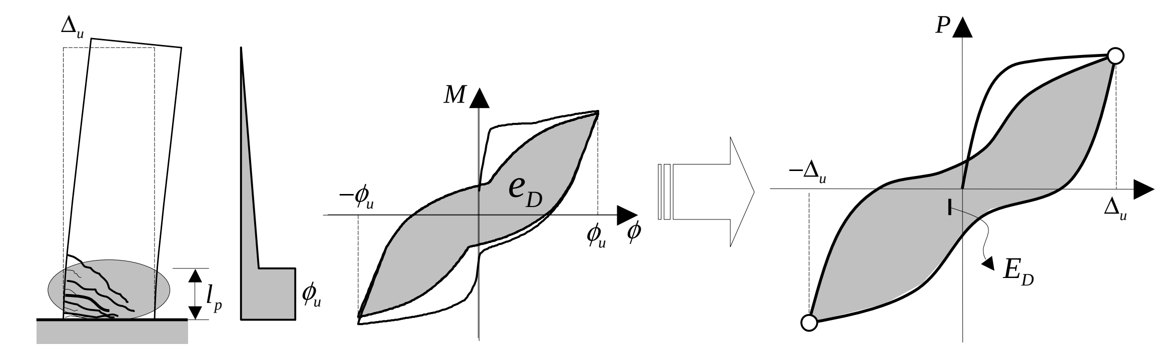

Fig. 9 Evaluation of energy dissipation capacity for R/C member

where l_p = length of the plastic hinge. The length of a plastic hinge at the base is approximately $h/2$. [2] When plastic hinges are developed at both ends of a member, the energy dissipation capacity of the member is the sum of energy dissipated at the both hinges.

Damping Modification Factor

In the present study, equations for estimating the damping modification factor of a member was developed to compare with the empirical ones used in the CSM, though actually in the Capacity-Spectrum-Method damping modification factor is used to estimate the energy dissipation capacity of a structure.

Fig. 10 shows the idealized cyclic curves developed by the elasto-plastic. According to Priestley [7], yield curvature ϕ_y of a cross-section can be approximately estimated, regardless of the amount and arrangement type of re-bars:

$$\phi_y = \alpha_{ST} \frac{\varepsilon_y}{h} \tag{7}$$

where h = depth or diameter of the cross-section, α_{ST} = modification factor accounting for variations of the yield curvature with the type of member and the shape of cross-section: α_{ST} = 2.00 for structural walls, 2.12 for columns with rectangular cross-section, 2.35 for columns with circular cross-section, and 1.70 for beams with rectangular cross-section.

The energy dissipation capacity e_{kh} based on the kinematic hardening behavior is calculated as

$$e_{kh} = 4M\left(\phi_u - \phi_y\right) = 4M\phi_y\left(\mu_\phi - 1\right) \tag{8}$$

where M = moment-carrying capacity, μ_ϕ = curvature ductility (= ϕ_u / ϕ_y).

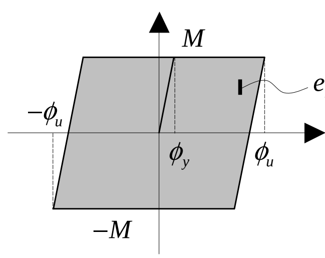

Fig. 10 Cyclic curves by elasto-plastic behavior of R/C members

The damping modification factor of reinforced concrete members can be defined as

$$\kappa = \frac{E_D}{E_{kh}} = \frac{e_D l_p}{e_{kh} l_p} = \frac{e_D}{e_{kh}} \tag{9}$$

By using Eq. (5), (8), and (9), the damping modification factor is defined as

$$\kappa = R_B\left(\frac{\rho f_y bh^2}{M}\right)\left(\frac{\mu_\phi}{\mu_\phi - 1}\right)\left[(1-p)\left(\frac{h_s}{2h} - \frac{1}{\alpha_{ST}\mu_\phi}\right) + p\left(\frac{1}{2} - \frac{1}{\alpha_{ST}\mu_\phi}\right)^2\right] \tag{10}$$

Verification of the Proposed Method

Table 2 compares the results of a variety of experiments and the values predicted by the proposed method. The dimensions and material properties for each specimen are presented in references.[8~13] The energy dissipation capacities and the damping modification factors are presented in the table. In the Capacity-Spectrum-Method, the damping modification factor is fixed to prescribed values in accordance with the expected energy dissipation capacity (Fig. 2), but in the proposed method it varies ranging from 0.314 to 0.693, depending on the design parameters. The average and the standard deviation of the ratio of energy dissipation capacity are 0.984 and 0.084, respectively. The values for ratio of the damping modification factor are 0.991and 0.085. In the present study, as mentioned, several simplifications were used to develop a practical method: Energy dissipated by concrete was neglected, and the strain profiles in the web of the cross-section were simplified. Furthermore, deformations due to shear-action, bond-slip, and pedestal rotation that might affect the energy dissipation capacity were not included. However, the comparisons presented in Table 2 showed that despite of such negative effects of the simplification, the proposed method predicts well the dissipated energy and the damping modification factor.

Table 2 Comparisons between experimental and analytical results

Specimen	Re-searchers	Type	Section shape**	Shear span ratio	Axial comp. $P/A_g f'_c$	Prediction		Experiments		Ratios of prediction to experiment	
						E_D***(1)	κ(2)	E_D(3)	κ(4)	(1)/(3)	(2)/(4)
88-32-RV10-60*	Brown & Jirsa [8]	Beam	R	5.00	0.00	13940	0.691	12710	0.693	1.097	0.997
88-35-RV10-60*		Beam	R	5.00	0.00	18430	0.693	16850	0.752	1.094	0.922
66-35-RV10-60*		Beam	R	5.00	0.00	8115	0.654	8086	0.751	1.004	0.871
OIN	Han&Lee[9]	Col.	R	4.55	0.28	1511	0.314	1500	0.322	1.007	0.975
N4	Cheok & Stone [10]	Col.	C	3.00	0.10	4179	0.510	4546	0.498	0.916	1.024
N5		Col.	C	3.00	0.20	4044	0.439	4784	0.460	0.845	0.954
N6		Col.	C	6.00	0.10	2760	0.503	3220	0.536	0.857	0.938
A1	Wehbe et. Al. [11]	Col.	R	3.83	0.10	57070	0.434	53880	0.450	1.056	0.964
A2		Col.	R	3.83	0.24	45900	0.405	46000	0.404	0.998	1.000
B1		Col.	R	3.83	0.09	66000	0.452	66940	0.489	0.986	0.924
B2		Col.	R	3.83	0.23	62090	0.404	66770	0.426	0.930	0.948
BG-3	Saatchioglu & Grira [12]	Col.	R	4.70	0.20	10600	0.348	11810	0.345	0.898	1.009
BG-5		Col.	R	4.70	0.47	16110	0.433	17040	0.413	0.945	1.048
BG-6		Col.	R	4.70	0.46	15860	0.435	15860	0.359	1.000	1.212
BG-7		Col.	R	4.70	0.47	16420	0.434	17910	0.418	0.917	1.038
BG-8		Col.	R	4.70	0.24	16260	0.424	13390	0.361	1.178	1.175
RW1	Thomsen & Wallace [13]	Wall	R	3.12	0.10	11860	0.384	12490	0.424	0.950	0.906
RW2		Wall	R	3.12	0.07	11860	0.378	11560	0.402	1.026	0.940

*Asymmetric cyclic tests **R: rectangular C: circular ***kN-mm

In the proposed equations, contribution of the lateral re-bars confining the core concrete was not included in the estimation of the energy dissipation capacity (per load cycle). Since the stress and strain of ties and stirrups are developed only by the concrete in compression, the stress and strain of the lateral re-bars remain in tension during repeated cyclic loadings. Therefore, the confining re-bars do not experience full cycles of strain history during cyclic loading repeated at specific displacements, and as the result, they dissipate little energy. For the reason, the effect of the confining re-bars on the energy dissipation capacity (per load cycle) was neglected in the present study. However, both the lateral re-bars and the confined concrete dissipate energy during loading increasing displacements.

APPLICATION OF THE PROPOSED METHOD

The simplified method to estimate the energy dissipation capacity of the flexure-dominated R/C member was applied to the nonlinear static and dynamic analysis. Fig. 11 and Table 3 present the configuration of the R/C frame, dimensions of each member, and material properties. Two lateral load profiles of triangular distribution and uniform distribution for the nonlinear static analysis were used as shown in Fig. 11. El Centro 1940(PGA=0.319g) and Northridge CA 1994(PGA=0.412g) were used as the earthquake record for the analysis.

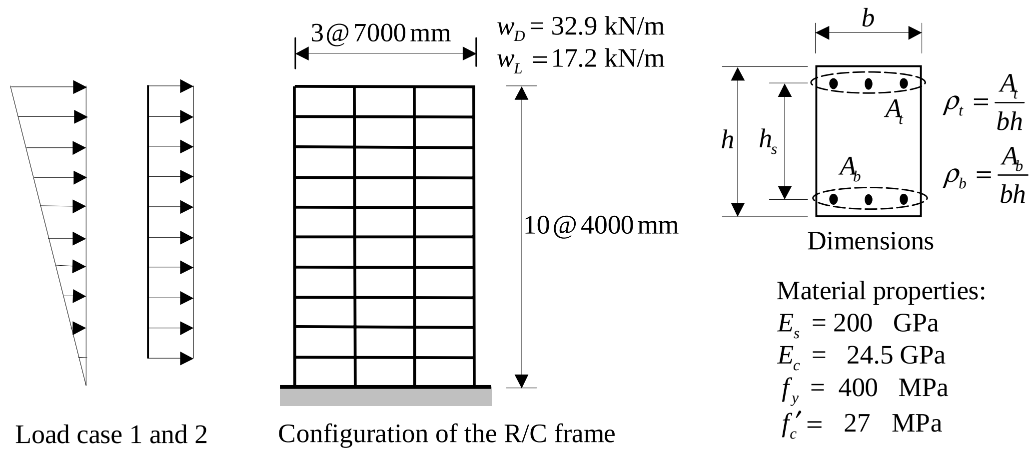

Fig. 11 10-story R/C frame for the nonlinear static and dynamic analysis

Table 3 Dimension and properties of beams and columns

Member		Width b mm	Depth h mm	Distance between re-bars h_s mm	Flexural reinforcement near the beam-column joints	
					ρ_t %	ρ_b %
Columns	1~3 Floors	700	700	610	1.00	1.00
	4~6 Floors	600	600	510	1.00	1.00
	7~10 Floors	500	500	410	1.00	1.00
Beams	All floors	400	600	520	1.00	0.75

The Capacity-Spectrum-Method was used for nonlinear static analysis. The proposed method and the empirical method proposed in ATC-40 were used to estimate the energy dissipation capacity. In the proposed method, as shown in Fig. 12, the energy capacity curve presenting the relation of the top displacement of the structure and the energy dissipated by complete cyclic behavior was constructed. In the energy capacity curve, the variation of energy dissipation capacity is defined by the function of displacement. In the CSM, the damping modification factor is fixed to a prescribed value. On the other hand, in the proposed method, the energy dissipation capacity varies depending on the design parameters and the displacement.

For time-history nonlinear analysis, energy-based bilinear cyclic model was developed. (Fig. 12) The model was devised so as to dissipate the same energy as the actual behavior during complete load cycle though the unloading- reloading behavior is different from the actual one.

The top displacements and base shears obtained by the CSM and dynamic analysis were presented in Table 4. For the dynamic analysis, the maximum responses during seismic behavior were presented. As presented in the table, the proposed method using the simplified method predicts better those of the nonlinear dynamic analysis, regardless of the lateral load profiles and earthquake records.

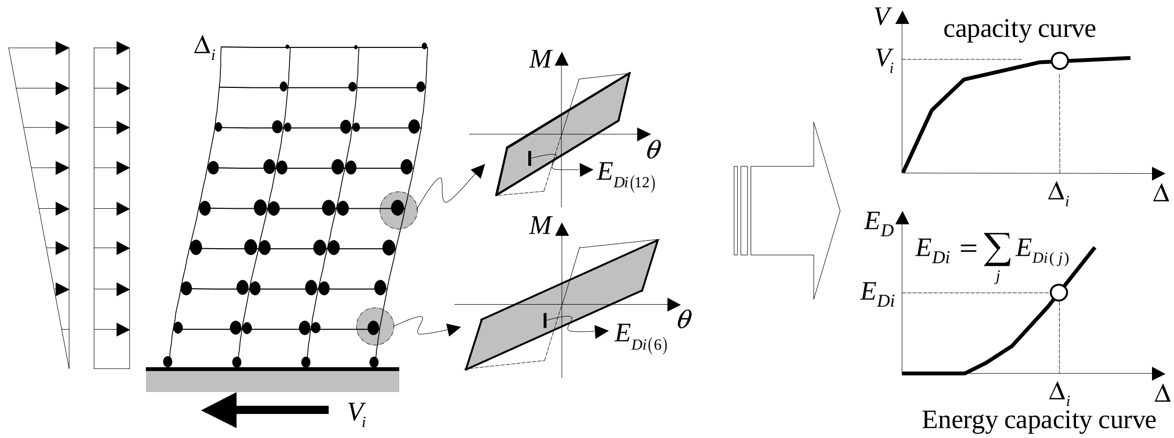

Fig. 12 Energy capacity curve for the capacity spectrum method

Table 4 Results by nonlinear static and dynamic analysis

		Proposed analysis		ATC-40's method*		Nonlinear dynamic analysis
		Load case 1	Load case 2	Load case 1	Load case 2	
El Centro 1940	Top disp.(mm)	242	240	223	202	248
	Base shear(kN)	886	1106	873	1057	1191
Northridge CA 1994	Top disp. (mm)	298	328	279	290	357
	Base shear(kN)	919	1189	909	1156	1394

* κ was used as 0.67

CONCLUSIONS

Nonlinear numerical analysis was performed to study the energy dissipation capacity of flexure-dominated reinforced concrete members. The behavioral characteristics of the members were studied, and the variations of the stress and strain profiles of re-bars occurring during cyclic loading were investigated. The major findings of the present study are summarized as follows.

1) Concrete which is a brittle material does not dissipate energy significantly during repeated cyclic loading. Therefore, the energy dissipation of the reinforced concrete member is almost the same as the energy dissipated by flexural re-bars arranged in the member.

2) Energy dissipation capacity of RC members can be determined by the amount of re-bars and the differential stains that the re-bars experience during cyclic loading.

3) The members with the same amount and arrangement of re-bars have almost the same energy dissipation capacity, regardless of the magnitude of the axial force applied to the member.

4) Therefore, the energy dissipation capacity of a flexure-dominated member can be calculated using the hypothetical cross-section subject to pure bending, neglecting the compressive force actually applied.

Based on the findings, a practical method for estimating the energy dissipation capacity and the damping modification factor was developed and verified by the comparisons with existing experiments. The proposed method can accurately estimate the energy dissipation capacity considering the reinforcement ratio and arrangement, axial compression, and ductility, without knowing the overall cyclic curve complicated by stiffness degradation and pinching. The proposed method is applicable to the existing nonlinear static and dynamic analysis.

ACKNOWLEDGEMENT

This research was financially supported by the Korea Earthquake Engineering Research Center and the Ministry of Construction & Transportation of South Korea, and the authors are grateful to the authorities for their support.

REFERENCES

1. ATC, "Seismic evaluation and retrofit of concrete buildings", *ATC-40*, Applied Technology Council, Redwood City, California, 1996
2. Building Seismic Safety Council, "NEHRP guidelines for the seismic rehabilitation of buildings", *FEMA-273*, Federal Emergency Management Council, Washington, D.C, 1997
3. S. Okamoto, S. Shiomi, and K. Yamabe, "Earthquake Resistance of Prestressed Concrete Structures", *Proceedings*, Annual Convention, AIJ, January. 1976, pp. 647-665
4. B. P. Sinha, Kurt H. Gerstle, and Leonard G. Tulin, "Stress-Strain Relations for Concrete under Cyclic Loading", *ACI Journal, Proceedings*, Vol.61, No.2, February. 1964, pp. 195-212
5. M. Seckin, "Hysteretic behavior of cast-in-place exterior beam-column sub-assembles", Ph. D. Thesis, University of Toronto, 1981, 266 pp.
6. H. Park and R. E. Klingner, "Nonlinear Analysis of RC Members Using Plasticity with Multiple Failure Criteria," *Journal of Structural Engineering, ASCE*, Vol.123, No.5, 1997, pp.643-651.
7. M. J. N. Priestley, "Performance Based Seismic Design", *Proceedings of the 12th World Conference on Earthquake Engineering*, Auckland, New Zealand, Jan. 30-Feb. 4, 2000
8. R. H. Brown and J. O. Jirsa, "Reinforced Concrete Beams under Load Reversals", *ACI Structural Journal*, Vol.68, No.5, 1971, pp. 380-390.
9. S. Han and L. Lee, "Seismic Behavior of OMRCF Columns", *Journal of the Korea Concrete Institute*, Vol. 14, no. 2, 2002, pp.199-206.
10. G. S. Cheok and W. C. Stone, "Behavior of 1/6-Scale Model Bridge Columns Subjected to Inelastic Cyclic Loading", *ACI Structural Journal*, Vol.87, No.6, 1990, pp. 630-638.
11. N. I. Wehbe, M. S. Saiidi, and D. H. Sanders, "Seismic Performance of Rectangular Bridge Columns with Moderate Confinement", *ACI Structural Journal*, Vol.96, No.2, 1999, pp. 248-258.
12. M. Saatchioglu and M. Grira, "Confinement of Reinforced Concrete Columns with Welded Reinforcement Grids", *ACI Structural Journal*, Vol.96, No.4, 1999, pp. 29-39.
13. J. H. Thomsen and J. W. Wallace, "Displacement-based design of RC structural walls: An experimental investigation of walls with rectangular and T-shaped cross-sections", Report No. CU/CEE-95/06